Volume 2, Number 1, 2025, 32-42

DOI: 10.71350/3062192528



Article

# High electrocatalytic activity and stability of Pt/TNT-RuO<sub>2</sub>

Qi Lv¹, Fanen Zeng², Zhen Tan¹, Yaning Zhang¹, Xun Yang¹, Bing Xu²

- <sup>1</sup> Dalian Jiaotong University, School of Transportation Engineering, Dalian, China
- <sup>2</sup> Dalian Jiaotong University, School of Materials Science and Engineering, Dalian, China

#### **Abstract**

In recent years, the high cost and limited stability of platinum-based catalysts in proton exchange membrane fuel cells (PEMFCs) have emerged as critical challenges hindering their widespread commercialization. TiO2 nanotubes (TNT), characterized by its one-dimensional hollow structure, high specific surface area, and chemical inertness, effectively anchors platinum nanoparticles and inhibits their migration and agglomeration. The incorporation of RuO<sub>2</sub> not only enhances the conductivity of the support but also promotes electronic synergy with platinum, thereby significantly improving both catalytic activity and stability. TNT-RuO2 was synthesized by integrating alkaline hydrothermal synthesis with the wet chemical method, thereby optimizing the dispersion of platinum and forming a strong metal-support interaction (SMSI). The synergistic oxygen reduction catalysis and high conductivity of RuO2 can compensate for the low catalytic activity of the catalyst caused by the insufficient conductivity of TNT. This composite carrier system not only mitigates carbon carrier oxidation and degradation through the corrosion resistance of TiO2 but also inhibits platinum Ostwald ripening by leveraging the stable oxidation state of RuO2. Research has confirmed that the electrochemical active surface area (ECSA) of Pt/TNT-RuO<sub>2</sub> is 60.5 m<sup>2</sup>·g<sup>-1</sup>, compared to 44.7 m<sup>2</sup>·g<sup>-1</sup> for Pt/C. After 10,000 cycles of accelerated stress testing, the EASA of the composite carrier catalyst decreased by only 33.9%, significantly lower than the 40.3% decay rate observed for Pt/C. This innovation offers a promising new approach for developing high-stability and cost-effective PEMFC catalysts.

#### **Article History**

Received 13.12.2024 Accepted 05.03.2025

#### Keywords

Titanium dioxide nanotubes; catalyst; stability; strong metal– support interaction

### Introduction

As global energy consumption continues to rise and environmental conditions deteriorate, the development of alternative and sustainable energy sources has become an urgent priority (Yang et al., 2013; Andújar & Segura, 2009). Furthermore, the exacerbating greenhouse effect and the critical shortage of non-renewable fossil fuels have significantly intensified the demand for cleaner and more efficient energy conversion technologies (Chu &Majumdar, 2012; Jin et al., 2018). Among various energy conversion devices, PEMFCs have garnered significant attention from researchers globally due to their high energy conversion efficiency, environmental friendliness, rapid start-up, and quiet operation (Tan et al., 2024; Yang et al., 2019). These advantages significantly contribute to mitigating the energy and environmental crises. Furthermore, hydrogen energy possesses an exceptionally high energy storage density

Corresponding Author Bing Xu ☑ Dalian Jiaotong University, School of Materials Science and Engineering, Dalian 116028, China

(142 MJ·kg<sup>-1</sup>) and can be directly utilized in fuel cells to generate electricity through chemical reactions. During this process, the only byproduct is water. Therefore, the critical role of hydrogen in future global energy supply has been widely acknowledged. Consequently, its large-scale application can effectively mitigate issues such as the energy crisis, environmental pollution, and global warming (Outlook, 2010; Staffell et al., 2019). PEMFCs technology is a crucial pathway for achieving the widespread utilization of hydrogen energy. Hydrogen fuel cells convert chemical energy from hydrogen and oxygen into electrical energy while simultaneously producing clean water as a byproduct and generating heat (Wei et al., 2020; Yang et al., 2013).

PEMFCs primarily consists of the membrane electrode assembly (MEA), bipolar plates (BPP), and external circuit. The MEA acts as the central component for the transport of electrons, protons, and gases, as well as the interface where electrochemical reactions occur, such as the oxygen reduction reaction (ORR) and hydrogen oxidation reaction (HOR). The performance of the MEA critically determines the overall performance, lifespan, and cost of the PEMFCs. The membrane electrode assembly (MEA) is a three-in-one component that integrates the proton exchange membrane (PEM), catalyst layer (CL), and gas diffusion layer (GDL) through hot pressing (Chen et al., 2024). The catalyst layer (CL) is further divided into an anode catalyst layer and a cathode catalyst layer. The cathode catalyst layer operates under harsh conditions, including high pressure and a strongly oxidizing environment. Consequently, ORR catalyst must possess excellent stability, which is a fundamental requirement for effective catalyst design (Aminudin et al., 2023; Banham et al., 2018). Currently, precious metals such as Pt and Pd are considered the most effective catalysts for enhancing the otherwise sluggish ORR kinetics, owing to their unique electronic structures. Although several non-precious metal catalysts have been developed as alternatives to Pt, significant efforts are still required to enhance their overall performance. In this context, enhancing the intrinsic activity of platinumbased catalysts and reducing platinum usage remain the most effective strategies. Traditional platinum nanoparticle-based catalysts are characterized by low platinum utilization and deactivated active sites (Giddaerappa et al., 2022; Zeng et al., 2012). Under dynamic conditions, the traditional carbon carrier is inevitably subject to corrosion in an instant, leading to a reduction in both catalytic activity and conductivity. This corrosion can also cause Pt nanoparticles to agglomerate and detach from the carbon surface (Li et al., 2021). Therefore, developing platinum-based catalysts with enhanced platinum utilization, superior activity, and improved stability has become one of the primary research focuses in PEMFCs.

A strong interaction typically exists between the supported metal and the carrier. This interaction not only enhances the anchoring of metal nanoparticles by the carrier but also modifies the local coordination environment and electronic structure of the metal on the surface (Giordano et al., 2010; Xu et al., 2022). Metal oxides serve as suitable carriers that can facilitate the uniform growth of Pt micro-nuclei and enhance the uniform dispersion of Pt particles. Due to its excellent corrosion resistance and electrochemical stability in both acidic and alkaline electrolytes, as well as its SMSI effect, this material has been extensively investigated (Cheng et al., 2017). The SMSI effect significantly influences the electronic structure of the supported metal, thereby markedly altering its catalytic activity, selectivity, and stability. Traditionally, this effect has frequently been observed during the hightemperature reduction of noble metal nanoparticles supported on metal oxides such as CeO<sub>2</sub>, TiO<sub>2</sub>, and tungsten oxide (WO<sub>x</sub>) (Maiyalagan & Viswanathan, 2008; Wang et al., 2023). Notably, the incorporation of transition metals can reduce the amount of Pt, thereby

controlling costs and enhancing intrinsic catalytic activity (Xia et al., 2022). Yang et al. (2013) previously reported that CrN exhibits excellent chemical and electrochemical stability in acidic solutions. They also found that the electrochemical activity and stability of Pt/CrN catalysts surpass those of Pt/C catalysts.

The unique crystal structure of titanium dioxide results in the separation of oxygen atoms (oxygen ions) within the lattice, leading to the formation of oxygen vacancies (Ovs) (Proch et al., 2017). These Ovs enhance the adsorption of oxygen-containing species on the oxide surface. On the other hand, both oxides are also readily available. Furthermore, compared to traditional carbon supports, titanium dioxide exhibits a stronger interaction with Pt, leading to enhanced catalytic performance (Xu et al., 2005). Titanium dioxide nanotubes possess a larger specific surface area compared to XC-72 and titanium dioxide nanoparticles. Their tubular structure provides a greater number of active sites for Pt NPs, facilitating more uniform deposition. Additionally, this structure enables faster electron transfer. Furthermore, as a carrier for Pt NPs, TNTs can efficiently disperse metal particles and exhibit strong metalsupport interactions. Esfahani et al. (2018) loaded Pt nanoparticles onto TNTs-Mo, demonstrating significantly higher ORR activity and stability compared to commercial Pt/C catalysts. This enhanced performance is primarily attributed to the confinement effect of TNTs, which effectively inhibits the agglomeration of Pt nanoparticles. Sebastian et al. (2021) prepared platinum thin film catalysts on acetylene-treated titanium dioxide nanotube array, which exhibited significantly higher ORR activity compared to commercial Pt/C catalysts. Studies have shown that the electrical conductivity and catalytic performance of these catalysts can be further optimized through doping with nitrogen, carbon, or transition metal elements (Ru, Pt). Specifically, the high conductivity of RuO<sub>2</sub> enhances catalytic activity, while its superior stability and corrosion resistance delay catalyst degradation.

This study synthesized heterogeneous composite TiO<sub>2</sub> nanotubes via an alkaline hydrothermal method and prepared TNT-RuO<sub>2</sub> using the sol-gel method. Subsequently, the Pt/TNT-RuO<sub>2</sub> catalyst was synthesized via the polyol method. To comprehensively characterize this catalyst, we employed various techniques, including transmission electron microscopy (TEM), X-ray diffraction (XRD), X-ray photoelectron spectroscopy (XPS), Brunauer-Emmett-Teller surface area analysis (BET), and electrochemical testing.

#### Method

### **Experimental Materials**

The following chemicals were used as received: titanium dioxide (TiO<sub>2</sub>, Aeroxide P25, Acros Organics), ruthenium chloride hydrate (RuCl<sub>3</sub>·xH<sub>2</sub>O, 35–40% Ru, Shanghai Aladdin Biochemical Technology Co., Ltd.), chloroplatinic acid hexahydrate (H<sub>2</sub>PtCl<sub>6</sub>·6H<sub>2</sub>O, Shanghai Aladdin Biochemical Technology Co., Ltd.), Potassium hydroxide (KOH, Tianjin Kemiou Chemical Reagent Co., Ltd.), Ethylene glycol (CH<sub>2</sub>OH)<sub>2</sub>, Xilong Scientific Co., Ltd.), Sodium hydroxide(NaOH, Tianjin Kemiou Chemical Reagent Co., Ltd.). All aqueous solutions were prepared with 18.2 M deionized water from a Millipore water system.

### **Synthesis of Titanium Dioxide Nanotubes**

The synthesis was carried out by the hydrothermal method. Specifically, 1g of titanium

dioxide was mixed with 75ml of 10M sodium hydroxide solution and ultrasonicated for 1 hour. Then, it was poured into the inner liner of a polytetrafluoroethylene high-pressure reactor. The hydrothermal reaction was conducted at 130°C for 24 hours. After the reaction was completed, the white precipitate was washed until the pH was approximately 7 and then dried for 8 hours at 400°C for calcination.

### Synthesis of Composite Metal Oxides.

TNT-RuO<sub>2</sub> was synthesized by wet chemical method. The mass ratio of TNT to RuO<sub>2</sub> was 1:2. A homogeneous solution was formed by ultrasonic treatment. Then, the pH was adjusted to neutral with 0.05M potassium hydroxide solution. The sample was dried at 60°C for 8 hours and calcined at 450°C for 3 hours. Thus, TNT-RuO2 was obtained.

### Pt/TNT-RuO2 Preparation of Catalyst.

The platinum catalyst was prepared by the polyol method. Ethylene glycol was used as the reducing agent and solvent. 30 mg of TNT-RuO2 was dispersed in 30 mL of ethylene glycol solution, and 5.3 ml of chloroplatinic acid ethylene glycol solution (19.8 mmol·L-1) was added to disperse uniformly. Then, the pH was adjusted to approximately 7 using 0.1 M NaOH solution, and the mixture was refluxed under cooling at 160°C for 3 hours. After cooling, the mixture was washed with deionized water and dried at 60°C for 8 hours. The Pt/C catalyst with XC-72R as the carrier was also prepared in the same way.

### **Physical Characterization**

XPS was carried out on the Thermo Fisher ESCALAB 250X spectrometer, which has a monochromatic Al K $\alpha$  X-ray source and a magnetic neutralizer operating at 90 W. This spectrometer is used for analyzing the chemical state of the catalyst. The sample's phase composition was determined by using the Dutch Panacore Empyrean X diffractometer (XRD) with a working voltage of 40 kV, current of 150 mA, scanning speed of 5 min-1, and a diffraction angle range of  $2\theta = 20^{\circ}$  -  $70^{\circ}$ . TEM analysis was conducted using the JEOL JEM-2100 F microscope which was operated at 200 kV.

#### **Electrochemical Testing of Catalysts**

A three-electrode system was employed, comprising a saturated calomel electrode (SCE) as the reference electrode, a platinum mesh as the counter electrode, and a glassy carbon electrode (GC, geometric area: 0.1256 cm<sup>2</sup>) as the working electrode. For the preparation of the working electrode, 5 mg of the catalyst sample was dispersed in a mixture of 2 mL anhydrous ethanol and 5 µL Nafion solution (5 wt%), followed by ultrasonic treatment to form a homogeneous catalyst ink. The ink was then deposited onto the GC electrode using a microsyringe and dried at ambient temperature. The Pt loading on the electrode was 0.16 mg·cm<sup>-2</sup>. Accelerated degradation tests (ADT) were conducted within the potential range of 0.60 - 1.00 V (vs. RHE) at a scan rate of 50 mV·s<sup>-1</sup>. CV measurements were performed in 0.5 M H<sub>2</sub>SO<sub>4</sub> electrolyte from -0.20 to 1.00 V (vs. SCE) at a scan rate of 50 mV·s<sup>-1</sup>. ECSA of Pt was calculated as follows:

$$ECSA = \frac{Q_H}{Q_{ref} \times L_{Pt}}$$

where QH denotes the charge associated with hydrogen adsorption, QREF represents the charge

required for monolayer hydrogen adsorption on Pt (210  $C \cdot (cm^2 \cdot Pt)^{-1}$ ), and  $L_{Pt}$  signifies the platinum loading in the cathode. ORR of the sample was evaluated using a rotating disk electrode (RDE) system. The measurements were conducted in 0.1 M HClO<sub>4</sub> at a scan rate of 10 mV·s-1 and a rotation speed of 1600 rpm, within the potential range of 0.20 to 1.20 V (vs. RHE).

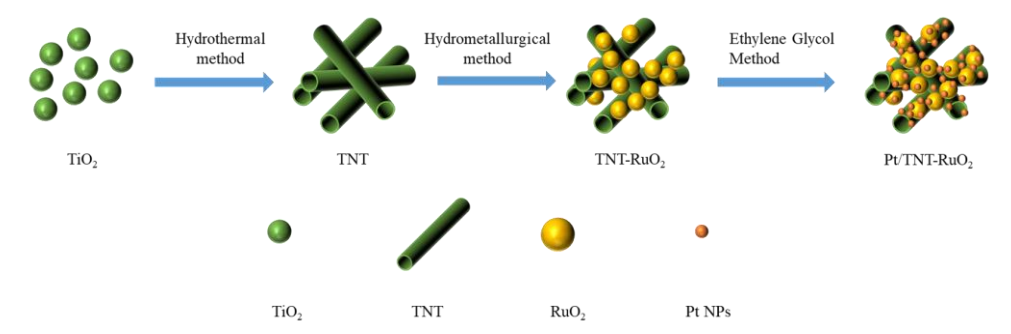
#### **Results and Discussion**

### Physical characterization

# Analysis of the synthesis process

TiO<sub>2</sub> powder was mixed with a concentrated alkali solution and subsequently placed in a high-pressure reactor. A hydrothermal reaction was performed at 130°C for 10 hours. Under these high-temperature and high-pressure conditions, the alkali solution etched the surface of TiO<sub>2</sub>, leading to its gradual dissolution and reassembly into a nanotube structure. This process can be detailed as follows: (1) Partial dissolution of titanium dioxide in an alkaline environment, resulting in the formation of titanate ([TiO(OH)<sub>3</sub>]); (2) Rearrangement of the titanate ions in the solution to form a layered structure; (3) The layered structure then curls into nanotubes due to surface tension effects.

The synthesis of TNT-RuO<sub>2</sub> employs RuCl<sub>3</sub> as the precursor, which undergoes hydrolysis and calcination to form RuO<sub>2</sub> nanoparticles on the surface of TNT. The process can be divided into three main stages: (1) Adsorption and hydrolysis of RuCl<sub>3</sub> on the TNT surface; (2) Crystallization and calcination to convert RuCl<sub>3</sub> into RuO<sub>2</sub>; (3) Formation of the composite structure. The high electrical conductivity of RuO<sub>2</sub> compensates for the insulating nature of TNTs, thereby significantly enhancing the electrochemical performance of the resulting composite material. The synthesis of Pt/TNT-RuO<sub>2</sub> via the polyol method facilitates the uniform deposition of Pt NPs on the TNT-RuO<sub>2</sub> composite support, as shown in Fig.1d.



**Scheme 1.** The synthesis flowchart of Pt/TNT-RuO<sub>2</sub>

#### TEM micrographs

Fig.1a presents the TEM image of TNT. The TiO<sub>2</sub> nanotubes synthesized via the alkaline hydrothermal method exhibit a well-defined tubular structure, with an inner diameter of approximately 4 nm, a wall thickness of about 1.3 nm, and an outer diameter of approximately 6.6 nm. Fig.1.c presents the TEM image of TNT-RuO<sub>2</sub>, demonstrating a uniform composite

structure of the two materials.Fig.1d shows the TEM image of Pt/TNT-RuO2, where Pt

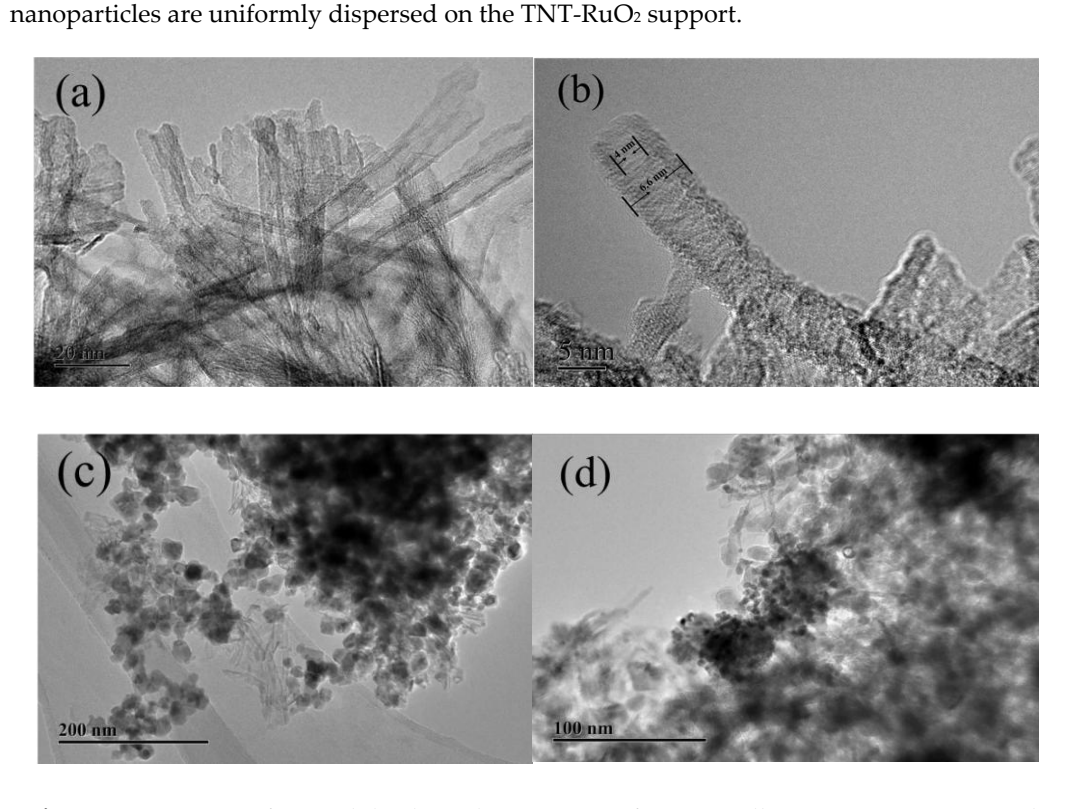


Fig.1 TEM patterns of (a) and (b) show the structure of TNT, (c) illustrates TNT-RuO<sub>2</sub>, and (d) depicts Pt/TNT-RuO<sub>2</sub>

#### XRD measurements

Fig.2a indicates that TiO<sub>2</sub> comprises both rutile (PDF#82-0514) and anatase (PDF#71-1166) phases. Following the synthesis of TNT via alkaline hydrothermal treatment, the crystal structure of TiO<sub>2</sub> transforms from anatase to titanate (PDF#36-0656). The XRD pattern of TNT exhibits two prominent peaks corresponding to the (401) and (020) crystal planes of titanate. During the subsequent preparation of TNT-RuO2, prolonged calcination at 450°C for 3 hours results in dehydration of TNT, leading to a structural transformation from titanate back to the more stable rutile phase. This phase transition enhances the electrochemical stability of the catalyst. Additionally, Fig.2a shows that RuO2 in Pt/TNT-RuO2 adopts a rutile structure, with three strong diffraction peaks corresponding to the (110), (101), and (211) crystal planes. Fig.2b presents the XRD patterns of Pt/C and Pt/TNT-RuO2. The diffraction peaks corresponding to the face-centered cubic (FCC) structure of Pt are observed at angles associated with the (111), (200), and (220) crystal planes (PDF#88-2343). The absence of additional impurity peaks confirms the high crystallinity of Pt. Notably, the sharp (111) peak, which is crucial for Pt catalytic activity, indicates excellent crystallinity of the Pt(111) plane. However, the Pt diffraction peaks in Pt/TNT-RuO<sub>2</sub> are less prominent due to the masking effect of the TiO<sub>2</sub> diffraction peaks.

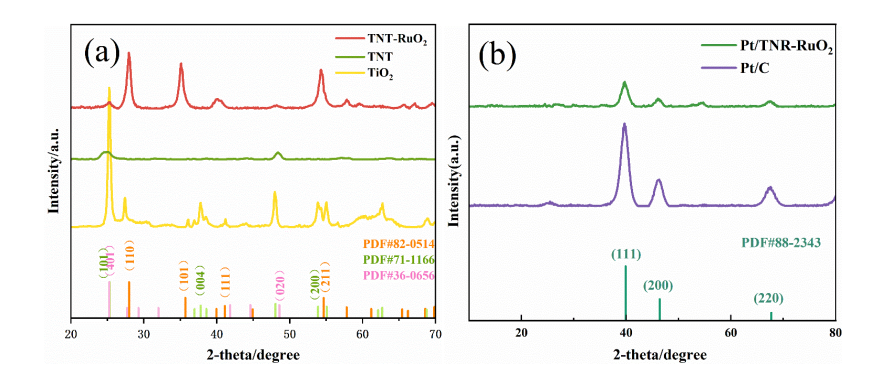
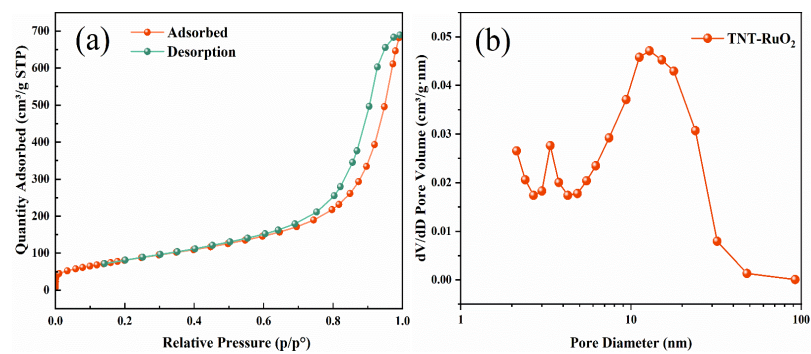


Fig.2. XRD patterns of (a) TNT and TNT-RuO<sub>2</sub>, and (b) Pt/TNT-RuO<sub>2</sub> and Pt/C

# Specific surface area measurement

The specific surface area and structural porosity are critical factors influencing the performance of ORR catalysts. The nitrogen adsorption-desorption isotherms for all samples are presented in Fig.3a, while the pore size distribution, calculated using the BJH model, is shown in Fig.3b. The BET specific surface area of TNT-RuO<sub>2</sub> is 280.78 m<sup>2</sup>·g<sup>-1</sup>. A higher specific surface area facilitates the exposure of more active sites, thereby enhancing ORR activity Error! R eference source not found. (Xie et al., 2022). The samples exhibit IV-type isotherms with H3-type hysteresis loops, indicative of mesoporous structures, which are further confirmed by the pore size distribution curve (Fig.3b). The presence of abundant mesopores promotes efficient mass transport of reactants such as protons and O<sub>2</sub> molecules, preventing reaction rate decline due to micropore blockage and thus improving catalytic efficiency. Additionally, the high specific surface area of the mesoporous structure aids in the uniform dispersion of Pt NPs, reducing agglomeration and enhancing the stability of the catalyst.



**Fig.3.** (a) Nitrogen adsorption-desorption isotherm, (b) BJH pore size distribution diagram

### XPS measurements

XPS analysis was conducted to investigate the elemental composition and valence states of Pt/TNT-RuO<sub>2</sub> and Pt/C catalysts. Fig.4a shows the main peaks corresponding to O1s, Ti2p, Ru3d, and Pt4f for Pt/TNT-RuO<sub>2</sub>, as well as O1s, C1s, and Pt4f for Pt/C. Fig.4b shows The peak positions of Pt4f<sub>5/2</sub> and Pt4f<sub>7/2</sub> in Pt/TNT-RuO<sub>2</sub> are observed at 74.34 eV and 71.25 eV, respectively, which are shifted to lower binding energies by 0.31 eV and 0.19 eV compared

with those of Pt/C. This shift is attributed to SMSI between Pt and TNT-RuO2, leading to electron transfer from the support to Pt, thereby increasing the electron density of Pt. This change lowers the d-band center of Pt, weakening the adsorption strength of oxygencontaining species, enhancing ORR activity, and reducing the occupation of active sites by intermediate products, thus improving stability. The SMSI effect also enhances the antioxidant capability of Pt nanoparticles, reduces Pt dissolution and loss, delays Ostwald ripening, and prolongs the catalyst's service life.

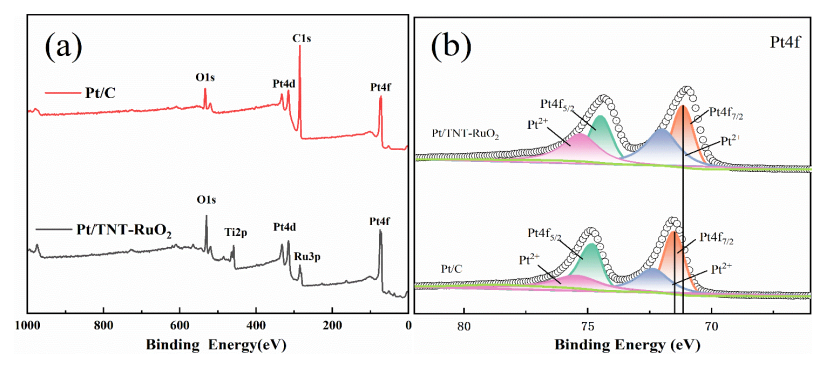


Fig.4. XPS spectra: (a) Full-scan XPS spectra of Pt/TNT-RuO<sub>2</sub> and Pt/C catalysts; (b) High-resolution Pt 4f XPS spectra of the same samples

### **Electrochemical Analysis**

# Analysis of ORR Activity of Catalysts

Fig.5 shows that Pt/TNT-RuO<sub>2</sub> exhibits superior ORR activity compared to Pt/C. Specifically, the initial potential and limiting current density of Pt/TNT-RuO2 are 1.028 V and 4.93 mA·cm <sup>2</sup>, respectively, which are higher than those of Pt/C (1.006 V and 4.62 mA·cm<sup>-2</sup>). Notably, the half-wave potential (E1/2) of Pt/TNT-RuO2 is 0.897 V (vs. RHE), positively shifted by approximately 15 mV relative to Pt/C (0.882 V). This positive shift in E1/2 indicates enhanced ORR activity for Pt/TNT-RuO<sub>2</sub>. The improved performance can be attributed to SMSI between Pt nanoparticles and TNT-RuO2, which facilitates electron transfer from the support to Pt, increasing its electron density. This effect lowers the d-band center of Pt, thereby weakening the adsorption strength of oxygen-containing species such as \*OOH, reducing the reaction energy barrier, and minimizing side reactions. Consequently, oxygen molecules are more readily activated on the catalyst surface, leading to enhanced ORR activity.

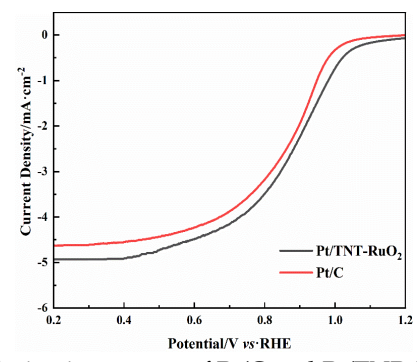


Fig.5. ORR polarization curves of Pt/C and Pt/TNR-RuO<sub>2</sub> catalysts

### Analysis of Catalyst Stability

Fig.6a,b show that the hydrogen adsorption regions for both Pt/TNT-RuO2 and Pt/C are within the range of -0.20 V to 1.00 V. According to Table 1, the initial ECSA of Pt/TNT-RuO2 (60.5 m²·g¬¹) is 1.74 times higher than that of Pt/C (44.7 m²·g¬¹). This significant difference can be attributed to the enhanced conductivity of TNT by RuO2, which increases the ECSA of Pt/TNT-RuO2 compared to Pt/C. After 10k ADT cycles, Pt/TNT-RuO2 retained 66.1% of its initial ECSA, whereas Pt/C retained only 59.7%. This superior retention is likely due to the better stability of TNT-RuO2 under acidic conditions and SMSI between Pt nanoparticles and TNT-RuO2. The SMSI effect reduces the dissolution rate and agglomeration tendency of Pt nanoparticles, weakens the adsorption strength of reaction intermediates, and minimizes surface poisoning, thereby enhancing the overall stability of the Pt/TNT-RuO2 catalyst.

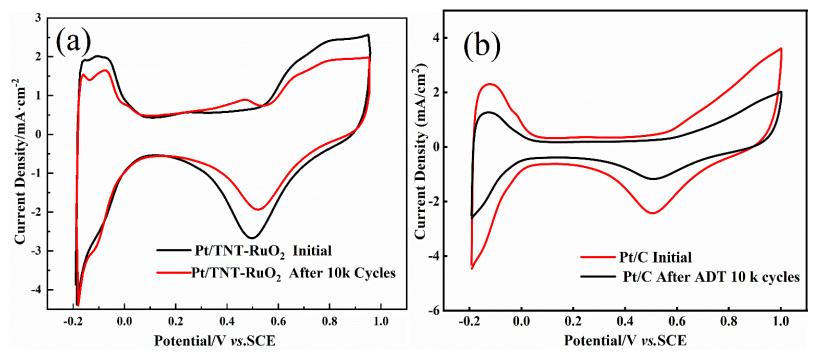


Fig.6. CV images before and after ADT are shown (a) Pt/TNT-RuO<sub>2</sub>, (b) Pt/C

Table 1. Parameter of Pt/C and Pt/TNT-RuO2 catalysts

Catalyst	Initial ECSA (m²·g⁻¹)	ECSA after 10k cycles (m²·g <sup>-1</sup> )	Maintenance rate after ADT (%)
Pt/C	44.7	26.7	59.7
Pt/TNT-RuO2	60.5	39.9	66.1

#### Conclusion

In recent years, the catalyst system for PEMFCs based on  $TiO_2$  nanotubes and  $RuO_2$  composites has demonstrated significant advantages in enhancing both the activity and stability of ORR. Studies have shown that the one-dimensional hollow structure and high specific surface area of  $TiO_2$  nanotubes effectively anchor platinum nanoparticles, inhibiting their migration and agglomeration. This not only optimizes the dispersion of platinum but also forms a SMSI, thereby improving the ORR activity of the catalyst. The incorporation of  $RuO_2$  enhances the conductivity of the carrier and significantly boosts catalytic performance through electronic synergy with platinum. In terms of stability, the corrosion resistance of  $TiO_2$  and the stable oxidation state of  $RuO_2$  effectively suppress platinum dissolution and Ostwald ripening. After 10k ADT, ECSA of the  $Pt/TNT-RuO_2$  composite catalyst retained 66.1% of its initial value, compared to only 59.7% for Pt/C. In conclusion, the  $TiO_2-RuO_2$  composite carrier system represents a promising direction for developing high-activity, high-stability, and cost-effective PEMFC catalysts, offering broad application prospects.

#### **Declarations**

*Acknowledgments:* Not applicable.

Authors' contributions: The authors contributed equally to the manuscript.

Competing interests: The author(s) declared no potential conflicts of interest with respect to the research, authorship, and/or publication of this article.

Funding: This research did not receive any specific grant from funding agencies in the public, commercial, or not-for-profit sectors.

Publisher's note: Advanced Research Journal remains neutral with regard to jurisdictional claims in published maps and institutional affiliations.

#### References

- Aminudin, M. A., Kamarudin, S. K., Lim, B. H., et al. (2023). An overview: Current progress on hydrogen fuel cell vehicles. International Journal of Hydrogen Energy, 48(11), 4371-4388.
- Andújar, J. M., & Segura, F. (2009). Fuel cells: History and updating. A walk along two centuries. Renewable and Sustainable Energy Reviews, 13(9), 2309-2322.
- Banham, D., Kishimoto, T., Zhou, Y., et al. (2018). Critical advancements in achieving high power and stable nonprecious metal catalyst-based MEAs for real-world proton exchange membrane fuel cell applications. Science Advances, 4(3), eaar7180.
- Chen, Y., Huang, Z., Yu, J., et al. (2024). Research progress of Pt-based catalysts toward cathodic oxygen reduction reactions for proton exchange membrane fuel cells. Catalysts, 14(9), 569.
- Cheng, X., Li, Y., Zheng, L., et al. (2017). Highly active, stable oxidized platinum clusters as electrocatalysts for the hydrogen evolution reaction. Energy & Environmental Science, 10(11), 2450-2458.
- Chu, S., & Majumdar, A. (2012). Opportunities and challenges for a sustainable energy future. Nature, 488(7411), 294-303.
- Esfahani, R. A. M., Gavidia, L. M. R., García, G., et al. (2018). Highly active platinum supported on Mo-doped titanium nanotubes suboxide (Pt/TNTs-Mo) electrocatalyst for oxygen reduction reaction in PEMFC. Renewable Energy, 120, 209-219.
- Giddaerappa, Manjunatha, N., Shantharaja, et al. (2022). Tetraphenolphthalein cobalt (II) phthalocyanine polymer modified with multiwalled carbon nanotubes as an efficient catalyst for the oxygen reduction reaction. ACS Omega, 7(16), 14291-14304.
- Giordano, L., Lewandowski, M., Groot, I. M. N., et al. (2010). Oxygen-induced transformations of an FeO (111) film on Pt (111): A combined DFT and STM study. The Journal of Physical Chemistry C, 114(49), 21504-21509.
- Jin, H., Guo, C., Liu, X., et al. (2018). Emerging two-dimensional nanomaterials for electrocatalysis. Chemical Reviews, 118(13), 6337-6408.
- Li, Z., Shen, T., Hu, Y., et al. (2021). Progress on ordered intermetallic electrocatalysts for fuel cells application. Acta Physico-Chimica Sinica, 37, 2010029.
- Maiyalagan, T., & Viswanathan, B. (2008). Catalytic activity of platinum/tungsten oxide nanorod electrodes towards electro-oxidation of methanol. Journal of Power Sources, 175(2), 789-793.

- Outlook, A. E. (2010). Energy information administration. Department of Energy, 92010(9), 1-15.
- Proch, S., Yoshino, S., Gunjishima, I., et al. (2017). Acetylene-treated titania nanotube arrays (TNAs) as support for oxygen reduction reaction (ORR) platinum thin film catalysts. *Electrocatalysis*, *8*, 351-365.
- Spasojević, M., Ribić-Zelenović, L., Spasojević, M., et al. (2021). Methanol electrooxidation on Pt/RuO2 catalyst. *Russian Journal of Electrochemistry*, *57*(7), 795-807.
- Staffell, I., Scamman, D., Abad, A. V., et al. (2019). The role of hydrogen and fuel cells in the global energy system. *Energy & Environmental Science*, 12(2), 463-491.
- Tan, M., Zhang, W., Liu, H., et al. (2024). Revolutionizing high-temperature polymer electrolyte membrane fuel cells: Unleashing superior performance with vertically aligned TiO2 nanorods supporting ordered catalyst layer featuring Pt nanowires. *Fuel*, 357, 130084.
- Wang, Y., Li, Z., Zheng, X., et al. (2023). Renovating phase constitution and construction of Pt nanocubes for electrocatalysis of methanol oxidation via a solvothermal-induced strong metal-support interaction. *Applied Catalysis B: Environmental*, 325, 122383.
- Wei, L., Shi, J., Cheng, G., et al. (2020). Pt/TiN–TiO2 catalyst preparation and its performance in oxygen reduction reaction. *Journal of Power Sources*, 454, 227934.
- Xia, J., Wang, B., Di, J., Li, Y., Yang, S.-Z., Li, H., & Guo, S. (2022). Construction of single-atom catalysts for electro-, photo- and photoelectro-catalytic applications: State-of-the-art, opportunities, and challenges. *Materials Today*, *53*, 217-237.
- Xie, X., Shang, L., Xiong, X., et al. (2022). Fe single-atom catalysts on MOF-5 derived carbon for efficient oxygen reduction reaction in proton exchange membrane fuel cells. *Advanced Energy Materials*, 12(3), 2102688.
- Xu, C., Zeng, R., Shen, P. K., et al. (2005). Synergistic effect of CeO2 modified Pt/C catalysts on the alcohols oxidation. *Electrochimica Acta*, *51*(6), 1031-1035.
- Xu, H., Zhao, Y., Wang, Q., et al. (2022). Supports promote single-atom catalysts toward advanced electrocatalysis. *Coordination Chemistry Reviews*, 451, 214261.
- Yang, L., Shui, J., Du, L., et al. (2019). Carbon-based metal-free ORR electrocatalysts for fuel cells: Past, present, and future. *Advanced Materials*, *31*(13), 1804799.
- Yang, M., Cui, Z., & DiSalvo, F. J. (2013). Mesoporous chromium nitride as a high performance noncarbon support for the oxygen reduction reaction. *Physical Chemistry Chemical Physics*, 15(19), 7041-7044.
- Yang, Z., Nie, H., Chen, X., et al. (2013). Recent progress in doped carbon nanomaterials as effective cathode catalysts for fuel cell oxygen reduction reaction. *Journal of Power Sources*, 236, 238-249.
- Zeng, J., Francia, C., Dumitrescu, M. A., et al. (2012). Electrochemical performance of Pt-based catalysts supported on different ordered mesoporous carbons (Pt/OMCs) for oxygen reduction reaction. *Industrial & Engineering Chemistry Research*, 51(22), 7500-7509.